Power-Aperture Resource Allocation for a MPAR With Communications Capabilities

Augusto Aubry, *Senior Member, IEEE*, Antonio De Maio, *Fellow, IEEE*, and Luca Pallotta, *Senior Member, IEEE*

***Abstract*—Multifunction phased array radars (MPARs) exploit the intrinsic flexibility of their active electronically steered array (ESA) to perform, at the same time, a multitude of operations, such as search, tracking, fire control, classification, and communications. This article aims at addressing the MPAR resource allocation so as to satisfy the quality of service (QoS) demanded by both line of sight (LOS) and reflective intelligent surfaces (RIS)-aided non line of sight (NLOS) search operations along with communications tasks. To this end, the ranges at which the cumulative detection probability and the channel capacity per bandwidth reach a desired value are introduced as task quality metrics for the search and communication functions, respectively. Then, to quantify the satisfaction level of each task, for each of them a bespoke utility function is defined to map the associated quality metric into the corresponding perceived utility. Hence, assigning different priority weights to each task, the resource allocation problem, in terms of radar power aperture (PAP) specification, is formulated as a constrained optimization problem whose solution optimizes the global radar QoS. Several simulations are conducted in scenarios of practical interest to prove the effectiveness of the approach.**

***Index Terms*—Dynamic resource allocation, single radio frequency (RF) platform integrated sensing and communication (ISAC), quality of service (QoS), resource management, reflective intelligent surfaces (RIS).**

NOTATIONS

symbol	description
$\boldsymbol{a}$	vectors (i.e., boldface)
$(\cdot)^T$	transpose operator
$(\cdot)^\dagger$	conjugate transpose operator
$\mathbb{R}^N$	set of N-dimensional vectors of real numbers
$\lvert\cdot\rvert$	modulus of a complex number
$\lVert\cdot\rVert$	Frobenius matrix norm
$\mathbb{E}[\cdot]$	statistical expectation
$f^{-1}(\cdot)$	inverse of a function $f(\cdot)$

Manuscript received 17 October 2023; accepted 10 January 2024. Date of publication 23 January 2024; date of current version 20 June 2024. The work of Augusto Aubry and Antonio De Maio was supported by the European Union through the Italian National Recovery and Resilience Plan (NRRP) of NextGenerationEU, partnership on "Telecommunications of the Future," CUP J33C22002880001, PE00000001 - Program "RESTART." The review of this article was coordinated by Prof. Yuan Wu. *(Corresponding author: Antonio De Maio.)*

Augusto Aubry and Antonio De Maio are with the Department of Electrical Engineering and Information Technology (DIETI), Università degli Studi di Napoli "Federico II," I-80125 Napoli, Italy (e-mail: augusto.aubry@unina.it; ademaio@unina.it).

Luca Pallotta is with the School of Engineering, University of Basilicata, 85100 Potenza, Italy (e-mail: luca.pallotta@unibas.it).

Digital Object Identifier 10.1109/TVT.2024.3357249

I. INTRODUCTION

MODERN radar systems are becoming more and more sophisticated due to the stressing requirement of multifunctionality which can be defined as the capability of performing and managing a multitude of different operations. This is becoming of vital importance both in the modern battlefield scenario, that could comprise a plethora of different challenging requirements so as to account for possibly different threats, and in civilian applications (e.g., for a radar in urban environment attempting to detect drones both in line of sight (LOS) and non line of sight (NLOS) as well as sending (possibly unidirectionally) communication signals to vehicular systems to convey potentially situational awareness information). Therefore, the multifunction phased array radar (MPAR) must perform different functions, such as search, tracking, fire control, classification, communication (COM), electronic counter-counter measure (ECCM), and also a multitude of tasks associated with each radar function [1]. To realize the aforementioned operations, the radar exploits the intrinsic flexibility provided by its active electronically steered array (ESA) antenna, which allows to synthesize multiple diverse beams, as well as to steer them into specific directions with negligible delays and without angular continuity requirements. Moreover, on the transmit side different waveforms, pulse repetition interval (PRI), dwells, and energy values can be used. The management of the system degrees of freedom is demanded to the radar resource manager (RRM), which assigns priorities to the functions and to the tasks composing them. Additionally, it performs their dynamic scheduling together with the parameter selection and optimization [2]. Accordingly, the mentioned functions and tasks are generally accomplished dedicating (to each of them) specific amounts of the available radar resources, for instance multiplexing them over different time intervals and/or looking angles. It is also clear that, in assigning the resource to each function/task, the RRM has to comply with physical and technical constraints, so as to appropriately handle the limited resource budget and the task induced performance constraints. In this respect, the RRM must decide, on the basis of the assigned priorities, for the optimal controllable resource allocation in order to guarantee the necessary quality for the high priority tasks at the expense of the others. Needless to say, in the scheduling process, once the resources to manage are specified, a tailored figure of merit for each involved task as well as the associated utility function must be defined to realize an optimized distribution of the available radar degrees of freedom [3]. Additionally, priorities

are represented via scalar weights associated with each task. Then, the optimization problem for the resource sharing is set-up on the basis of the above quantities, where the objective function that describes the satisfaction for the overall success of the radar mission is maximized [3]. In this respect, the RRM can use different optimization tools to perform resource allocation. Among them, it is worth mentioning the quality of service resource allocation method (Q-RAM) [4] and the continuous double auction parameter selection (CDAPS) [5], [6].

The Q-RAM consists of few steps to handle a constrained optimization problem for discrete parameter selection. In a nutshell, starting from the situation where the resource for each task is zero, it performs an iterative subdivision of the degrees of freedom to each task in the order specified by the highest to the lowest marginal utility. Once the available resource is entirely allocated, the algorithm ends. Other interesting applications of the Q-RAM within the framework of radar resource management can be found in [1], [7], [8], [9], [10], [11], [12], [13]. Analogously, the CDAPS models the tasks as agents, each of them having its own resource to utilize. Since, the total amount of resources for all tasks should not exceed a specific quantity, the problem is tackled through the application of a continuous double auction (CDA) market algorithm [2]. Some other interesting uses of the CDAPS related to the radar resource management problem can be found in [14], [15], [16]. Other studies devoted to the optimization of the power allocation in a distributed multiple input multiple output (MIMO) system performing both radar and communication functions have also been developed in the last years [17], [18], [19]. In particular, in [17], an optimization problem is formulated to reach as better as possible the desired performance in terms of target detection along with the desired data rate of the communication function. Moreover, in [18], the allocation paradigm is modified to boost the performance of the distributed MIMO system in terms of its low probability of intercept (LPI). Finally, in [19], the above described resource allocation is expanded to the context of multi-target tracking.

Unlike the mentioned references, in this article, a quality-of-service (QoS) optimization is developed for a suitable allocation of the resources in a MPAR system performing integrated sensing and communication (ISAC) activities, via a multitude of functions and tasks ranging from surveillance in both LOS and NLOS environments to possibly unidirectional data transmission operations. Specifically, this article is framed in the context of a single radio frequency (RF) ISAC platform where the resources of a common phased array are shared among different concurring tasks in a smart way so as to avoid mutual interference. This is a different operational mode as compared with the ISAC approaches developed in [20], [21], [22], [23], [24], [25], where the waveforms and/or reflective intelligent surfaces (RIS) elements are controlled for communication/sensing centric or co-design paradigms considering the sum or linear combination of the signal to interference plus noise ratio (SINR) for the different tasks as objective function. To this end, following the lead of [3], after defining parameters characterizing multiple search sectors, RIS-aided search, as well as multiuser COM tasks, their respective quality metrics and utility functions are introduced. Hence, the resulting resource allocation is formulated as a constrained optimization problem, where the power-aperture product (PAP) is distributed to allow maximization of the overall QoS. Notably, the formulated resource allocation problem is characterized by a non-convex objective function also only available in an implicit form. Hence the resulting optimization program can only be tackled via numerical methods. Several case studies of practical interest are analyzed to demonstrate the validity of the approach.

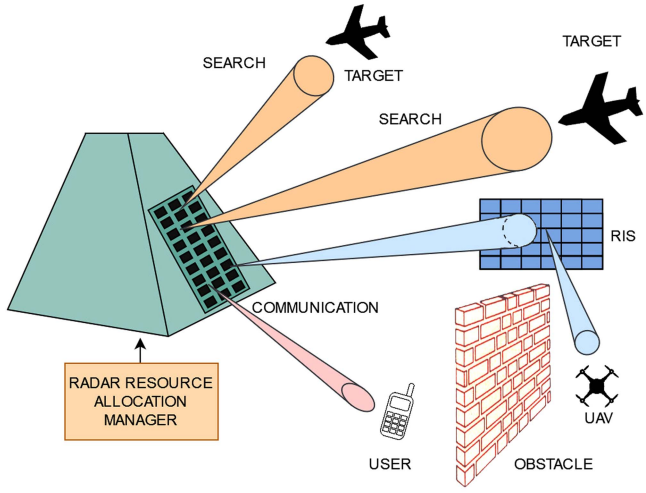

Fig. 1. Notional representation of a MPAR system performing surveillance in LOS situations, using RISs for NLOS search, as well as implementing a COM functionality.

The article is organized as follows. In Section II, the MPAR system is presented and the QoS optimization problem is formulated considering the PAP as degree of freedom. Then, in Section III the quality metrics are defined for each task together with their respective utility functions. The problem is particularized and solved for some case studies of practical interest in Section IV. Finally, some concluding remarks are given in Section V.

II. Problem Statement

In this article, a MPAR system equipped with an active ESA antenna is considered (see Fig. 1 for a notional illustration of the operating scenario). It is capable of performing multiple functions, e.g., just to mention a few, radar surveillance (search) in LOS scenarios, RIS-aided search in NLOS scenarios (a.k.a. detection *over the corner*), COM activities (possibly unidirectional) toward some users, tracking, and so on.

To allocate appropriately the resources required to each task, the radar employs a dynamic radar parameters assignment. In an ideal context, the system has the possibility to assign at each task the resources demanded to reach the desired performance. However, due to the limited availability, the radar system has to face with a suitable distribution of the degrees of freedom over the different tasks. Therefore in a MPAR, the resources at the radar disposal are not a-priori fixed as in the classic surveillance systems, but rather they are dynamically allocated during its operation on the basis of the specific mission and its

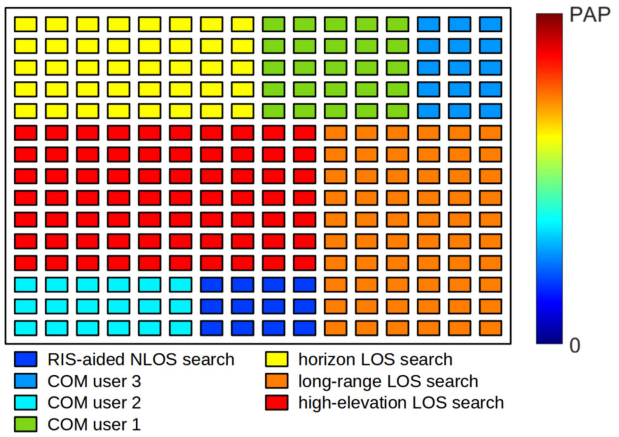

Fig. 2. Pictorial description of the PAP allocation to the different tasks of the active ESA.

actual state, as well as depending on some priorities associated with each task. From a practical point of view the active ESA is composed of many tiles each with a given PAP. They are clustered according to the requirements of the system tasks so that each group realizes an overall PAP value. A pictorial description of the concept can be seen in Fig. 2.

The PAP (defined as the product between the average transmitted power and the radar aperture) is considered as the limited resource that must be granted to perform the different tasks. Obviously, if the available PAP overcomes that needed to satisfy the requirements for all the active tasks, enough PAP is given to each of them. Nevertheless, being the PAP physically and practically limited, only a percentage of the resource demanded by each task can be, in general, allocated by the RRM at each schedule time. The aforementioned assignment is performed on the basis of a pool of figure of merits and utility functions depending, in general, on the specific resources to distribute as well as on the design and environmental parameters (that are not under control), say $\boldsymbol{\zeta}_i$, $i = 1, \ldots, L$, where L is number of independent tasks, $T = \{T_1, \ldots, T_L\}$ that must share a finite common resource. To proceed further, recall that the i-th task utilizes the allocated resource to achieve a specific QoS, quantified by a quality measure $q_i(PAP_i; \boldsymbol{\zeta}_i)$ tailored to the specific task. Therefore, the objective function for the resource allocation problem is obtained via the definition of a mapping among the L task qualities and the achieved utilities in order to measure the overall effectiveness of the MPAR mission. As a consequence, the RRM should find the optimal partition of PAP between tasks such that the weighted sum of their utilities is maximized [15, Chap. 3], [3, Chap. 5]. In this context, the task utility function provides the satisfaction level corresponding to the achieved task quality metric value. Moreover, to partially account for different degrees of relevance and priorities among the tasks, these utilities are suitably weighted in the formation of the overall RRM utility metric. In other words, denoting by $PAP = [PAP_1, PAP_2, \ldots, PAP_L]^T \in \mathbb{R}^L$ the vector containing as i-th entry the PAP attributed to the i-th task, $i = 1, \ldots, L$, the PAP distribution is obtained as the optimal solution to the following constrained optimization problem [3, Chap. 5], [44]

$$\begin{cases} & \max_{PAP} \; u(PAP) \\ \text{s.t.} & \sum_{i=1}^{L} PAP_i \leq PAP_{tot} \\ & PAP_i \geq PAP_{\min_i}, i = 1, \ldots, L \end{cases}, \tag{1}$$

where

$$u(PAP) = \sum_{i=1}^{L} w_i u_i(q_i(PAP_i; \boldsymbol{\zeta}_i)) \tag{2}$$

PAP_{tot} is the total amount of PAP available at the MPAR, $u_i(\cdot)$, $i = 1, \ldots, L$, is the utility function of the i-th task, whereas w_i, $i = 1, \ldots, L$, are the weights reflecting the priorities among the L tasks. Finally, $PAP_{\min_i}$, $i = 1, \ldots, L$, guarantees that the i-th task is accomplished with a minimum level of QoS. Note that, it is assumed $\sum_{i=1}^{L} PAP_{\min_i} \leq PAP_{tot}$, in order to ensure feasibility to the resource allocation problem.

Now, if the task utility function $u_i(q_i(PAP_i; \boldsymbol{\zeta}_i))$ is a continuous convex function of PAP_i, then the objective function is convex and hence the Karush-Kuhn-Tucker (KKT) conditions can be exploited to establish the optimal resource allocation [3, Chap. 5]. If the resource, quality and utility functions are available in a closed-form, then the KKT conditions can be solved analytically. However, it is often the case that the quality metrics do not possess a closed-form. In such a situation, even if the utilities exhibit a closed-form and the constraints are linear, the objective function is only available numerically, making the problem unsolvable in analytic form. As a consequence, the solution to the resource allocation problem can be only numerically obtained, as it is the case of the resource planning handled in this article.

The next section describes the task quality metrics together with their corresponding utilities herein considered for the dynamic PAP allocation paradigm described by (1).

III. Task Quality and Utility for QoS Resource Management

The allocation strategy formalized by Problem (1) depends on the considered figure of merits $q_i(\cdot;\cdot)$, and utility functions $u_i(\cdot)$, $i = 1, \ldots, L$. The goal of this section is to specify them, so as to concretely define the scheduling machinery.

A meaningful figure of merit for the surveillance functions (both in the LOS and NLOS scenarios) is provided by the cumulative detection range, denoted as R, that is the range where the cumulative probability of detection (P_d) is larger than or equal to a desired value [3], [13], [15], [26]. The cumulative P_d is indeed defined as the probability that a target is detected at least once in a given number of dwells [3], [26]. In fact, when a target enters in a search sector, its detection can be performed over multiple scans. Moreover, the cumulative P_d increases at each scan especially as the target approaches the radar.

Similarly, for the COM function, the quality metric can be defined as the communication range, indicated as R_{com}, corresponding to the maximum distance at which a minimum bit-rate can be conveyed reliably. These two metrics are deeply described in Sections III-A and III-B.

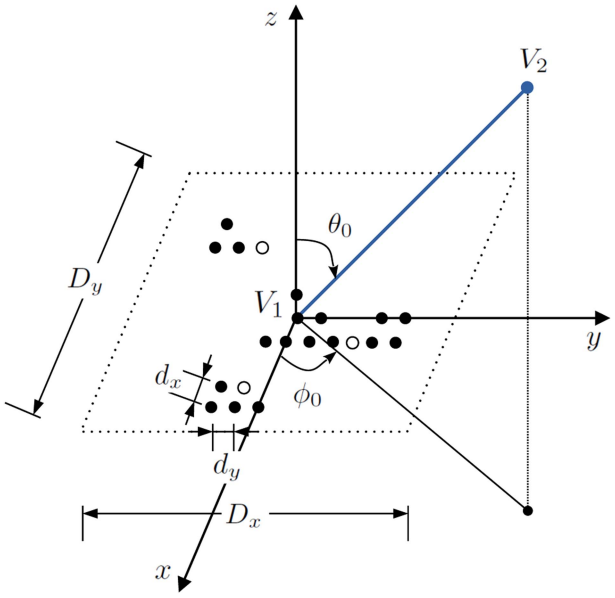

Fig. 3. Reference system of a generic planar array.

Before proceeding further, it is worth recalling the one-way link equation, which is useful for subsequent derivations.

Remark 1: Let us consider a source located at the point $V_1 \in \mathbb{R}^3$, transmitting an electromagnetic (EM) wave with a peak power of P_T and an antenna steered in the direction described by the azimuth and elevation angles ϕ_0 and θ_0, according to the coordinate system depicted in Fig. 3. Denoting by G_T the peak antenna gain when it points in the boresight direction, the spatial power density at point V_2 is

$$\mathcal{P}^{in} = \frac{P_T G_T}{4\pi R^2 L_s L_{\text{steer}}}, \tag{3}$$

where $R = \|V_2 - V_1\|$, i.e., the distance between the transmitter and the receiver, and L_s is the combined system operational loss [27]. Moreover, L_{steer} is the term accounting for the scanning gain loss of the steered antenna in the pointing direction[1] (θ_0, ϕ_0), which implicitly embeds the spatial selectivity in the antenna gain. In fact, as the pointing angles deviates from the boresight, the beam broadens while its peak drops out. The loss in peak gain due to scanning for a generic planar array depends on both the pointing direction (i.e., azimuth and elevation) and the single element radiating pattern. Practically, the values of these losses are off-line evaluated and then stored in a look-up table to be applied during radar's operation. However, in the particular case of a uniform rectangular array (URA) under some technical assumptions as for instance large array size and omnidirectional array elements, L_{steer} assumes a simplified approximated form, depending only on the elevation angle cosine [28], [29].

[1]It is worth to underline that, even if L_{steer} depends on the considered pointing angles, to simplify the notation, the dependence on (θ_0, ϕ_0) is omitted in the rest of the paper.

A. Search Task Quality Metric

Let us indicate with $P_d(R')$ the single-look P_d at range R', and assume that S is the number of scans the target needs to reach the range R from the pop-up range R_m. Hence, the respective cumulative P_d for the search sector of interest at range R is given by [26]

$$P_c(R|R_m) = 1 - \prod_{n=0}^{S-1} \left[1 - P_d\left(R_m - n v_r t_f - \Delta\right)\right], \tag{4}$$

with v_r the target radial speed, t_f the frame time (i.e., the time necessary to perform a single scan of the sector), and Δ a sample of a uniform random variable[2] in the interval $[0, v_r t_f]$, with $v_r t_f$ the distance traveled by the target in a single scan, modelling the initial target position in the corresponding radar cell. Note that, the functional dependence of the range on the pop-up range is $R = R_m - (S-1)v_r t_f - \Delta$. The single-look P_d can be evaluated once the desired false alarm probability, say P_{fa}, is set. More specifically, assuming a Swerling (SW) 0 (respectively a SW 1) model for the target amplitude and assuming a coherent integration of the pulses in a dwell, the single-look detection probability at range R' can be obtained as [27]

$$P_d(R') = Q_M\left(\sqrt{2\text{SNR}}, \sqrt{-2\log P_{fa}}\right) \quad \text{(SW0)} \tag{5}$$

and

$$P_d(R') = P_{fa}^{1/(1+\text{SNR})} \quad \text{(SW1)}, \tag{6}$$

where $Q_M(\cdot,\cdot)$ is the Marcum Q-function [30]. Note that, the functional dependence on the variable R' of the P_d is embedded in the expression of the coherent signal to noise ratio (SNR).

Let us now consider a radar located at point V_1 aimed at detecting a (possible) target at point V_2 in a LOS environment. To contextualize the cumulative P_d expression to the resource allocation process, it is necessary to particularize the result of Remark 1 (3) to the links V_1-V_2 and V_2-V_1. Accordingly, the SNR can be expressed as [27, eq. 2.17]

$$\text{SNR}^{\text{LOS}} = \frac{P_T G_T G_R \lambda_0^2 \sigma n_p}{(4\pi)^3 R_{\text{LOS}}^4 k_B T_s B L_s^{\text{LOS}} L_{\text{steer}}^{\text{LOS}}}, \tag{7}$$

where G_R is the receiving antenna peak gain, $R_{\text{LOS}} = \|V_1 - V_2\|$, T_s is the system noise temperature, L_s^{LOS} is the combined two-way system operational loss [27], $L_{\text{steer}}^{\text{LOS}}$ is the total scanning loss in the LOS scenario, σ is the target radar cross section (RCS), k_B is the Boltzmann's constant, λ_0 is the operating wavelength, and n_p is the number of integrated pulses in a dwell. Assuming a monostatic radar configuration using the same beam in transmission and reception, (7) can be arranged in the search-form of the radar range equation (RRE) [27]. To this end, recall that [27]

$$t_d = \frac{t_f}{M} = \frac{t_f}{\Omega A_e}\lambda_0^2, \tag{8}$$

where M is the number of beam positions to cover the solid angle search sector Ω and the effective area of the radar antenna

[2]Without loss of generality, Δ is set equal to zero in the next analyses.

A_e is related to the radar peak gain by [27]

$$G_T = 4\pi \frac{A_e}{\lambda_0^2}. \tag{9}$$

Hence, substituting (8)–(9) in (7), the search-form of the RRE (5)–(6) boils down to

$$\text{SNR}^{\text{LOS}} = PAP \frac{\sigma}{4\pi k_B T_s R_{\text{LOS}}^4 L_s^{\text{LOS}} L_{\text{steer}}^{\text{LOS}}} \frac{t_f}{\Omega} \tag{10}$$

where $PAP = P_{avg} A_e$, with P_{avg} the average transmit power. Before concluding the description of the LOS scenario, it is worth to underline that (10) implicitly assumes the absence of interference among the signals of the different concurring tasks. In fact, the system manager itself coordinates the entire pool of sub-systems and allocates the resources of its phased array to avoid mutual interference among the different spatial beams.

As to the NLOS scenario, encompassing a gapfiller RIS that aids the detection *over the corner* [31], let us indicate with V_1, V_2, and V_3 the positions of the radar, RIS, and target, respectively, and, accordingly, $r_{\text{NLOS}} = \|V_1 - V_2\|$ and $R_{\text{NLOS}} = \|V_2 - V_3\|$. Therefore, leveraging Remark 1, the expression for the SNR can be derived accounting for the multiple paths involved in the surveillance process, i.e., V_1-V_2, V_2-V_3, V_3-V_2, and V_2-V_1, along with the target RCS and the radiation patterns synthesized at the RIS equipment.[3] Specifically, the RRE assumes the form [31]

$$\text{SNR}^{\text{NLOS}} = \frac{G_T^2 G_{\text{RIS}}^2 A_{\text{RIS}}^2 \eta_{\text{RIS}}^2 \lambda_0^2 \sigma P_{avg} t_d}{r_{\text{NLOS}}^4 R_{\text{NLOS}}^4 (4\pi)^5 k_B T_s L_s^{\text{NLOS}} L_{\text{steer}}^{\text{NLOS}}}, \tag{11}$$

with L_s^{NLOS} the combined system operational loss in the NLOS case [27], $L_{\text{steer}}^{\text{NLOS}}$ the total scanning loss in the NLOS scenario. A_{RIS} is the RIS area, that for a uniform rectangular geometry can be expressed as $\delta_x \delta_y N_1 N_2$, with $\delta_x = \delta_y = \lambda_0/2$ the patch size along x- and y-direction, respectively, and N_1, N_2 the respective number of patches. Additionally, η_{RIS} is the RIS efficiency (assumed, for simplicity, common to all the patches), which accounts for taper and spillover effects [36]. Hence, the product $A_{\text{RIS}}\eta_{\text{RIS}}$ is the effective aperture of the RIS. Finally, G_{RIS} is the RIS peak gain.

The SNR of a RIS-aided search radar can be again expressed in terms of PAP. Precisely, substituting (8)–(9) in (11), the search-form of the RIS-aided RRE is

$$\text{SNR}^{\text{NLOS}} = \frac{PAP\, G_{\text{RIS}}^2 A_{\text{RIS}}^2 \eta_{\text{RIS}}^2 \sigma}{r_{\text{NLOS}}^4 R_{\text{NLOS}}^4 (4\pi)^3 k_B T_s L_s^{\text{NLOS}} L_{\text{steer}}^{\text{NLOS}}} \frac{t_f}{\Omega}. \tag{12}$$

Before concluding this section, it is now worth observing that a commonly reference value for the objective P_c is 0.9. For this reason, the corresponding cumulative detection range denoted by R_{90}^{LOS} for LOS tasks, can be expressed as

$$R_{90}^{\text{LOS}} = P_{c,\text{LOS}}^{-1}(0.9, R_m), \tag{13}$$

having denoted by $P_{c,\text{LOS}}^{-1}(x|R_m)$ the inverse of the function in (4) for the LOS case, i.e., when the SNR is dictated by SNR^{LOS} in (10). Analogously, for the NLOS search task

$$R_{90}^{\text{NLOS}} = P_{c,\text{NLOS}}^{-1}(0.9, R_m), \tag{14}$$

with $P_{c,\text{NLOS}}^{-1}(x|R_m)$ the inverse of the function in (4) for the NLOS case, i.e., when the SNR is given by SNR^{NLOS} in (12).

Note that (13) and (14) implicitly define the PAPs demanded to attain the desired QoSs for the surveillance tasks.

B. COM Task Quality Metric

The metric that describes the quality for a COM task is the maximum range, indicated as R_{com}, for which the channel capacity per bandwidth is equal to a specific value. Before evaluating R_{com}, let us consider the transmission of a signal composed by the superposition of $U \leq B^{\text{COM}} T^{\text{sym}}$ frequency (or code) orthogonal waveforms, $x_i(t), i = 1, \ldots, U$, to U COM receiving users, with B^{COM} the bandwidth reserved by the radar to COM operations, and T^{sym} the symbol interval. Then, the transmitted signal is

$$x(t) = \sum_{i=1}^{U} \sum_{h=0}^{N^{\text{sym}}-1} s_i(\phi_i, \theta_i) x_i(t - hT^{\text{sym}}) \alpha_i(h), \quad 0 \leq t \leq T^{\text{COM}}, \tag{15}$$

where $T^{\text{COM}} = T^{\text{sym}} N^{\text{COM}}$, N^{COM} indicates the number of symbols transmitted in each scheduled interval, $\alpha_i(h)$, $h = 0, \ldots, N^{\text{sym}} - 1$, accounts for the information symbols for the i-th user, and $s_i(\theta_i, \phi_i)$ is the transmit beamformer pointing toward the i-th user at position (θ_i, ϕ_i) w.r.t. the coordinate system centered at the transmitting antenna phase-center position.

Assuming an additive white Gaussian noise (AWGN) channel, with $w(t)$ the noise contribution, the signal acquired at the k-th receiver, with reference to the h-th symbol interval, can be expressed as

$$\begin{aligned} r_k(t) &= \boldsymbol{s}_k^{\dagger} \beta_k \boldsymbol{x}(t - \tau_k) + w(t) \\ &= \beta_k \sum_{i=1}^{U} \boldsymbol{s}_k^{\dagger} \boldsymbol{s}_i x_i(t - \tau_k) \alpha_i(h) + w(t), \end{aligned} \tag{16}$$

with $\boldsymbol{s}_k$ the steering vector in the direction (θ_k, ϕ_k), β_k the complex scaling factor accounting for channel propagation effects and receive antenna, and τ_k the propagation time of the k-th user. Note that, the functional dependence of $\boldsymbol{s}_k$ on (ϕ_k, θ_k) is omitted for brevity.

At receiver side, the samples of the incoming signal after matched filter operation to $x_k(t - \tau_k)$ becomes

$$\langle r_k(t), x_k(t - \tau_k) \rangle = \beta_k g_k \alpha_k(h) + w_k(h), \quad h = 0, \ldots, N^{\text{sym}} - 1, \tag{17}$$

where g_k is the transmitter beamformer complex gain in the direction (ϕ_k, θ_k) of the k-th user, and $\langle \cdot, \cdot \rangle$ denotes the inner product operator.

Finally, the channel capacity per bandwidth (expressed in bit/s/Hz) for the k-th user can be defined as [37], [38], [39]

$$C = \log_2 \left(1 + \text{SNR}_k^{\text{COM}}\right), \tag{18}$$

[3] It is assumed that a RIS realizes an appropriate beamforming, i.e., the parameter-settings of the RIS, such as its element phase shifts, are already suitably optimized to face with the assigned task. In this respect, some techniques for RIS phase-shift optimization can be exploited. The interested readers could refer to [32], [33], [34], [35], just to list a few.

where $\mathrm{SNR}_k^{\mathrm{COM}}$ is the SNR at the k-th COM user receiver.

Let us indicate with V_1 and V_2 the positions of the transmitter and the k-th COM user, respectively, and $R_{k,\mathrm{COM}} = \|V_1 - V_2\|$. According to Remark 1, the SNR in (18) can be computed with respect to the link V_1-V_2 as

$$\mathrm{SNR}_k^{\mathrm{COM}} = \frac{P_k |g_k|^2 |\beta_k|^2}{\sigma_k^2}, \tag{19}$$

where $P_k = \mathbb{E}[|\alpha_k|^2]$ is the transmitting power for the k-th communication link, and $\sigma_k^2 = k_B T_s^{\mathrm{COM}} B^{\mathrm{COM}}$ is the noise power at the k-th receiver, with T_s^{COM} and B^{COM} the respective noise system temperature and effective bandwidth. Let us observe now that

$$|g_k|^2 |\beta_k|^2 = \frac{G_T A_e^{\mathrm{rx},k}}{4\pi R_{k,\mathrm{COM}}^2 L_s^{\mathrm{COM}} L_{\mathrm{steer}}^{\mathrm{COM}}}$$

with $A_e^{\mathrm{rx},k}$ the effective area of the k-th user receiving antenna, L_s^{COM} the COM system operational loss, and $L_{\mathrm{steer}}^{\mathrm{COM}}$ the total scanning loss in the COM scenario. Hence, following the above definitions, SNR_k in (19) can be expressed in terms of PAP, i.e.,

$$\mathrm{SNR}_k = \frac{P_k |g_k|^2 |\beta_k|^2}{\sigma_k^2} = PAP_k \frac{A_e^{\mathrm{rx},k}}{\lambda_0^2 R_{k,\mathrm{COM}}^2 L_s^{\mathrm{COM}} L_{\mathrm{steer}}^{\mathrm{COM}} \sigma_k^2}. \tag{20}$$

Finally, denoting by C_{desired} the reference value for the objective channel capacity, its corresponding range, say R_{com}, is derived as follows

$$R_{\mathrm{com}} = \sqrt{\frac{PAP_k A_e^{\mathrm{rx},k}}{\lambda_0^2 L_s^{\mathrm{COM}} L_{\mathrm{steer}}^{\mathrm{COM}} \left(2^{C_{\mathrm{desired}}} - 1\right) \sigma_k^2}}. \tag{21}$$

C. Task Utility

Once the task quality metrics are defined, the joint optimum allocation of tasks' PAPs can be computed as the optimal solution to the QoS optimization problem in (1). In this respect, the RRM needs to map the quality metrics to their corresponding utilities. As a matter of fact, the utility provides a description of the degree of satisfaction reached when each task is completed. A possible way to define the utility for the i-th considered task is through the following model [13]

$$u_i(q_i(\mathrm{PAP}_i, \boldsymbol{\zeta}_i)) = u_i(R_c) = \begin{cases} 0, & R_c < R_{t_i} \\ \frac{R_c - R_{t_i}}{R_{o_i} - R_{t_i}}, & R_{t_i} \le R_c \le R_{o_i} \\ 1, & R_c > R_{o_i} \end{cases} \tag{22}$$

where R_{t_i} and R_{o_i} are the threshold and objective ranges of the i-th task, respectively. Moreover, R_c denotes the quality metric for the specific task,[4] viz. the cumulative detection range R_{90} or the communication range R_{com}, respectively. Obviously, at ranges lower than the threshold, the utility is zero, because the considered ranges are too close to the MPAR making the function useless. Then, the utility increases linearly as the range increases since it reaches its objective value, beyond which it saturates to 1. It is worth noticing that both the threshold and objective range are task depending parameters.

D. Optimization Algorithm

To obtain a solution to the challenging and non-convex resource allocation problem defined in (1) the iterative optimization algorithm in [40] is exploited. Therein, the interior-point approach to constrained optimization[5] is employed, which amounts to solve a sequence of approximate minimization problems which include non-negative constrained slack variables (as many as the inequality constrains of the original problem) and equality constraints. These are easier to solve than the original inequality-constrained problem and are handled either via a direct solution of the corresponding KKT equations (via a linear approximation, i.e. a Newton step) or via a conjugate gradient method [41], [42], [43]. Specifically, the algorithm first attempts to pursue a direct step. If it cannot be applied, it employs a conjugate gradient approach. Notably, one relevant case where the direct step is not exploited arises when the approximate problem is not locally convex near the current iterate.

From an implementation point-of-view, the solution algorithm is based on the availability of an oracle (realized via a tailored numerical procedure) that provides the values for the objective function for each choice of the parameters as well as with the desired accuracy. This is indeed possible thanks to the analytic expressions which in implicit form rule the relationships among the objective and the different design parameters.

It is fundamental to remark that no optimality claims can be done being the problem at hand non-polynomial (NP) hard, in general. Nevertheless, the proposed technique leads to a solution that is a-posteriori practically effective, as shown by the results reported in Section IV.

IV. Case Studies

In this section, some case studies for the pondered MPAR system performing both search and COM operations are analyzed. Specifically, the resource allocation is done after defining the priority weight for each task as well as the overall PAP available at the system. Problem (1) is solved using the Mathworks Matlab *Quality-of-Service Optimization for Radar Resource Management* [44] which performs a constrained minimization of a given objective function. The focus is on a scenario involving seven different tasks: three refer to search in LOS scenarios (shortly referred to as Horizon, Long-range, and High-elevation, respectively), three COMs with three different users, and a RIS-aided search to tackle a NLOS surveillance.

A. Parameter Setting

Tests conducted in this article refer to a MPAR operating in X-band with its central frequency $f_0 = 10$ GHz. Now, before providing the definition of all the involved parameters, for each considered task, the antenna coverage sector is specified in terms

[4]Note that, the dependence on $\boldsymbol{\zeta}_i$ is omitted, being the environmental parameters fixed in the addressed problem.

[5]Maximizing a utility is tantamount to minimizing the associated cost, given by the opposite of the utility.

TABLE I
LOS SEARCH TASKS SIMULATION PARAMETERS

parameter	value		
	Horizon	Long-range	High-elevation
t_f (s)	0.5	6	2
T_s (K)	913	913	913
v_r (m/s)	250	250	250
σ (m^2)	1	1	1
P_{fa}	10^{-6}	10^{-6}	10^{-6}
L_s^{LOS} (dB)	22	19	24
$L_{\text{steer}}^{\text{LOS}}$ (dB)	0.01	0.13	2.31

TABLE II
COM TASKS SIMULATION PARAMETERS

parameter	value		
	user 1	user 2	user 3
T_s^{COM} (K)	916	916	916
B^{COM} (MHz)	40	40	40
$A_e^{\text{rx},k}$ (m^2)	0.7×10^{-3}	0.7×10^{-3}	0.7×10^{-3}
L_s^{COM} (dB)	27	27	27
$L_{\text{steer}}^{\text{COM}}$ (dB)	0.15	0.62	0.87

of angle limits, and observation range. In particular, the angular parameter setup specifies the following sector limits:

- Horizon, $[-45, 45]$ degrees in azimuth and $[0, 4]$ degrees in elevation,
- Long-range, $[-30, 30]$ degrees in azimuth and $[0, 30]$ degrees in elevation,
- High-elevation, $[-45, 45]$ degrees in azimuth and $[30, 45]$ degrees in elevation.
- COM functions, $[-45, 45]$ degrees in azimuth and $[0, 45]$ degrees in elevation.
- RIS-aided, $[15, 20]$ degrees in azimuth and $[28, 32]$ degrees in elevation.

Additionally, the maximum range of interest (a.k.a. range limit) for each task is set as:

- Horizon, 40 km,
- Long-range, 70 km,
- High-elevation, 50 km.
- COM user 1, 45 km,
- COM user 2, 55 km,
- COM user 3, 65 km,
- RIS-aided, 4 km.

Other parameters for the three search tasks are summarized in Table I, for the three COM tasks are reported in Table II, and for the RIS-aided (a uniform rectangular RIS is considered during the analysis) search in Table III. It is worth highlighting that, a practical example for a search radar, which in part agrees with Table I, is that of a ground surveillance system SHORAD (short range air defence) for air reconnaissance. In fact, it can possibly transmit with a low effective radiated power, and can also operate above C-band, where free-space loss is high [45]. Finally, in all the conducted simulations herein presented, $PAP_{\min_i}$, $i = 1, \ldots, L$, is set to 0 W $\cdot$ m^2 unless otherwise stated.

TABLE III
RIS-AIDED SEARCH TASK SIMULATION PARAMETERS

parameter	value
t_f (s)	2
T_s (K)	913
v_r (m/s)	50
σ (m^2)	0.02
P_{fa}	10^{-6}
L_s^{NLOS} (dB)	19
G_{patch} (dB)	4
δ_x, δ_y	$\lambda_0/2$
N_1, N_2	101
η_{RIS}	0.8
r_{NLOS} (km)	1
$L_{\text{steer}}^{\text{NLOS}}$ (dB)	1.25

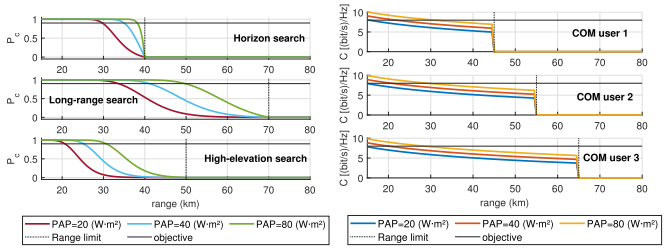

(a)

(b)

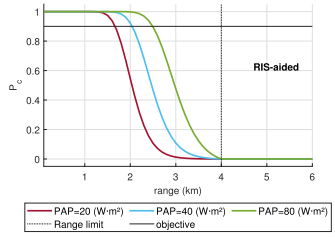

(c)

Fig. 4. Cumulative P_d for the LOS (subfigure a) and NLOS (subfigure c) search tasks, and channel capacity per bandwidth (subfigure b) for the COM tasks, considering multiple per-task PAP allocations.

B. Case Study 1

The first case study refers to a MPAR with the parameters described in Section IV-A assuming a SW1 fluctuating target model for both the high-speed targets considered in three LOS search functions and for the small unmanned aerial vehicle (UAV) to be detected via RIS-aided surveillance. In this scenario, the cumulative P_d (4) and channel capacity per bandwidth (18) are shown in Fig. 4 versus range for three different values of the PAP assigned to each task, viz. $[20, 40, 80]$ W $\cdot$ m^2. Subfigures a) and c) of Fig. 4 refer to search tasks, whereas subfigure b) to COM operations.

For all the subfigures of Fig. 4, the corresponding range limit is also shown. QoS values beyond these limits are not of interest and set to zero as is evident for the COM tasks. Moreover, the desired value for the cumulative P_d (i.e., $P_{c_{\text{desired}}} = 0.9$), and for the channel capacity per bandwidth (i.e., $C_{\text{desired}} = 8$ bit/s/Hz) are highlighted in the same graph. Hence, the corresponding range values R_{90} and R_{com} are derived for each PAPs, numerically solving the equations $P_c^{\text{LOS}}(R_{\text{LOS}}|R_m) - P_{c_{\text{desired}}} = 0$,

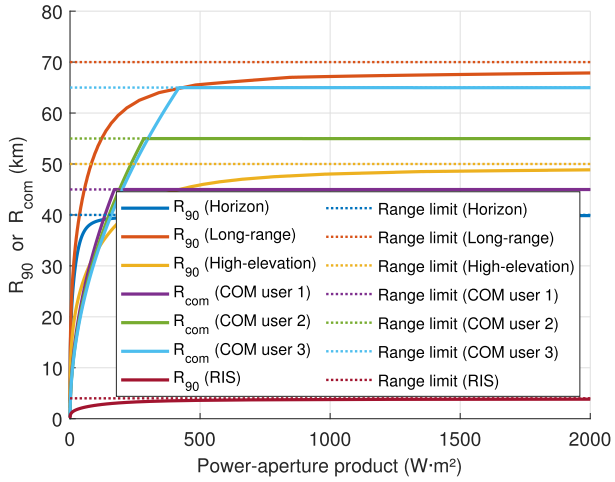

Fig. 5. Task quality versus assigned resource for the different radar operations.

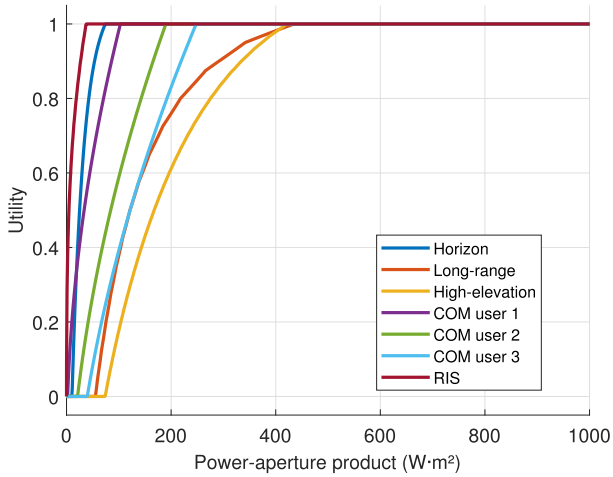

Fig. 7. Utility versus resource for the different radar operations.

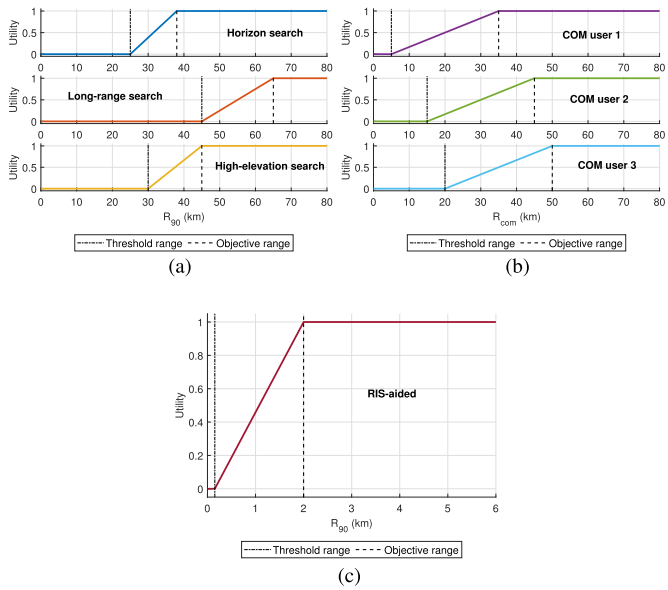

Fig. 6. Utility functions for LOS search tasks (subfigure a), COM (subfigure b) and NLOS search operation (subfigure c) tasks.

$P_c^{\text{NLOS}}(R_{\text{NLOS}}|R_m) - P_{c_{\text{desired}}} = 0$, and $C(R_{\text{COM}}) - C_{\text{desired}} = 0$ with respect to the variable R_{LOS}, R_{NLOS}, and R_{COM}, respectively. These results are reported in Fig. 5, where the task quality is shown versus the allocated resource to any specific task, i.e., $PAP_i = PAP_h$, for any $i, h = 1, \ldots, 7$. As expected, increasing the assigned PAP produces a growth of the task quality until its limit is attained. This means that if the current value of PAP for a specific task is such that the range limit is almost attained, it is no longer required to allocate additional resource, since it does not produce appreciable improvements in the corresponding quality.

In Fig. 6 the utility functions for the above considered tasks are reported, particularizing the general form given by (22) setting the objective ranges to $R_o = [38, 65, 45, 35, 45, 50, 2]$ km and the threshold ranges to $R_t = [25, 45, 30, 5, 15, 20, 0.153]$ km for the three search (subfigure a), three COM (subfigure b) and RIS-aided (subfigure c) tasks, respectively. Note that, the threshold ranges are set following different requisites for each task under study. Precisely, for the LOS search functions, it is the minimum range beyond which the mission is considered failed, because the target is too close to the radar for successfully activate subsequent actions. As to COM tasks, the communication is assumed valid within a specific segment between two circles centered at the radar location, i.e., with the user located beyond a minimum distance from the radar until the possible maximum range of interest. For the RIS-aided detection, the threshold range is set equal to the far field distance (FFD) that can be computed as [31]

$$R_{\text{FFD}} = \frac{2\left(\max(\delta_x N_1, \delta_y N_2)\right)^2}{\lambda_0}. \tag{23}$$

Therefore, for the parameter values summarized in Table III, FFD computed via (23) is approximately 153 m. Finally, the objective ranges, that allow to reach the maximum utility, are set according to the mission requirements.

Moreover, using the above-described utility functions, the PAP (namely, the resource) can be mapped to the utility space as shown in Fig. 7. From the inspection of these curves, it appears that the Long-range search, High-elevation search, COM user 2 and 3 need to exploit non negligible PAP values to reach non-zero utilities, viz., 56, 74, 22, and 40 W $\cdot$ m^2, respectively. Conversely, the rest of the tasks are capable of reaching nonzero utilities with very low values of assigned PAP. Moreover, the Long-range and High-elevation search functions demand high PAP values to obtain the maximum utility, i.e., 422 and 435 W$\cdot$m^2. Interestingly, the operation that requires the minimum PAP value to attain the maximum utility is the RIS-aided search with PAP of 38 W $\cdot$ m^2.

Now, the first simulation analyzes the case where the resource allocation is performed under normal operational conditions (i.e., no optimization is performed) in which the maximum utility is reached for each of the operating tasks. Hence, each task exploits all the necessary resource (i.e., the maximum utility PAP) to fulfill its demanded nominal objective, viz. cumulative P_d and/or channel capacity per bandwidth. To highlight this

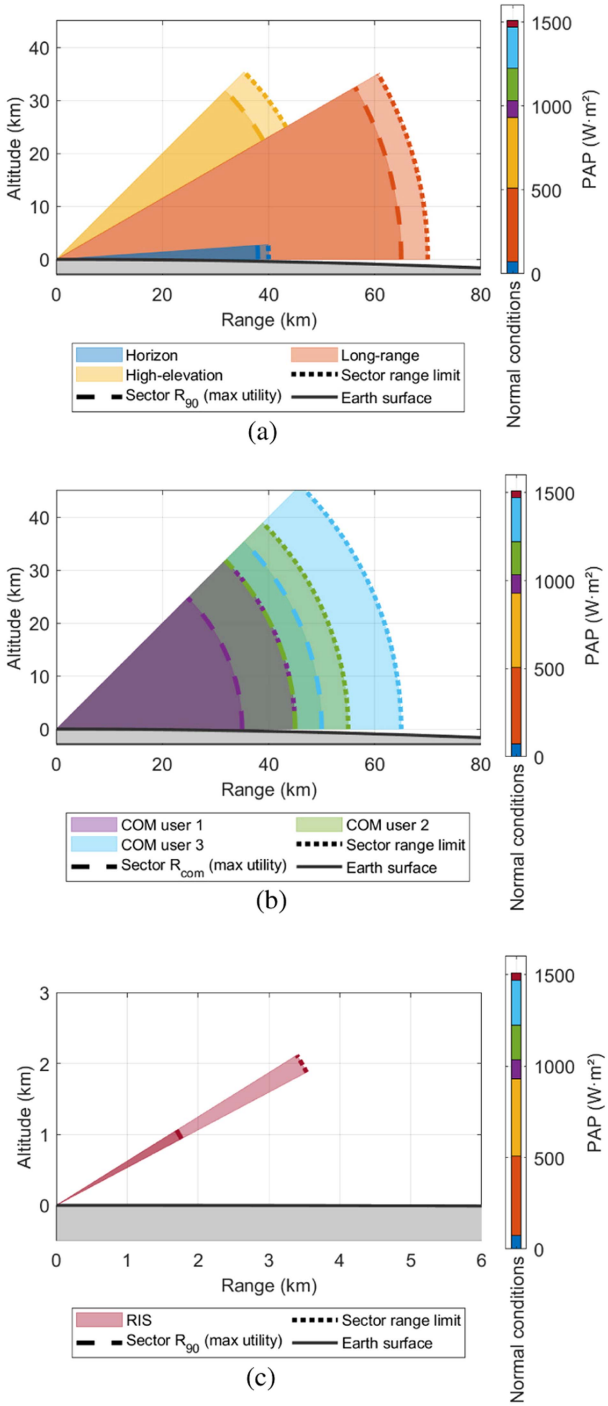

Fig. 8. Resource allocation of MPAR LOS search tasks (subfigure a), COM activities (subfigure b), and NLOS search operation (subfigure c) under normal operational conditions. The line style of each attribute inherits the color of the corresponding task.

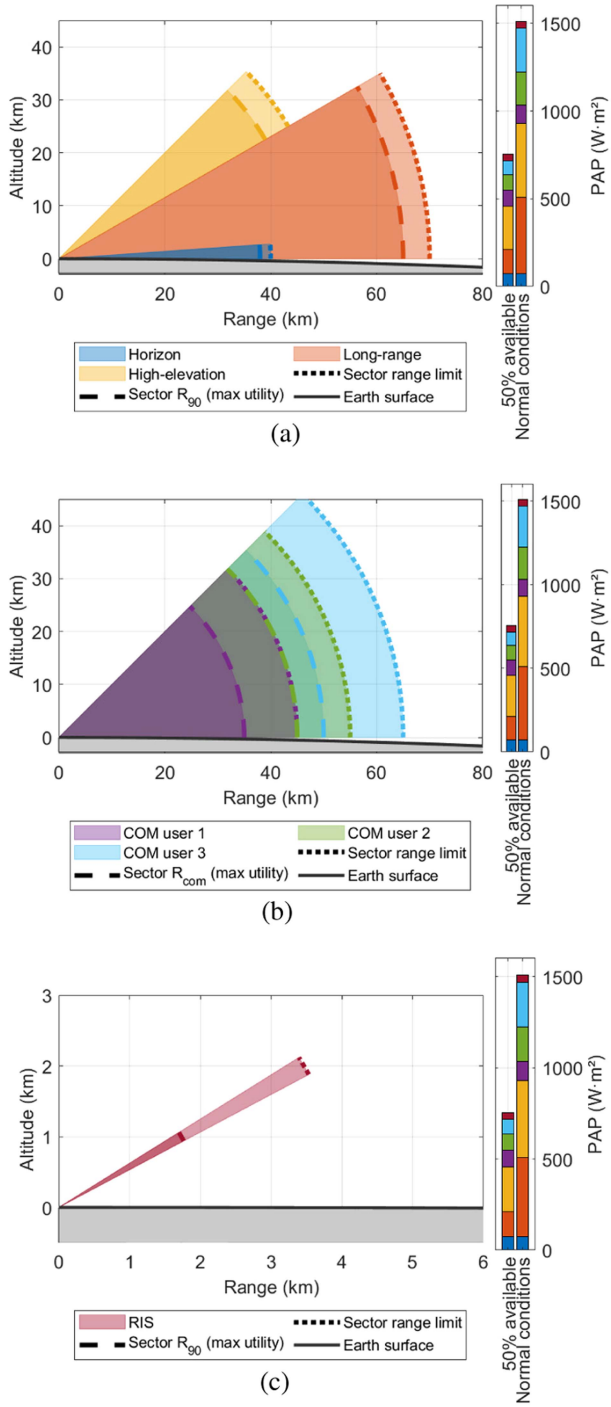

Fig. 9. Resource allocation of MPAR LOS search tasks (subfigure a), COM activities (subfigure b), and NLOS search operation (subfigure c), with priority weights $\mathrm{w} = [0.4, 0.1, 0.2, 0.06, 0.06, 0.06, 0.12]^T$.

distribution, Fig. 8 proposes a graphical representation of the antenna coverage sectors as well as the objective value R_{90} (respectively R_{com}) for the different radar operations. Subfigures refer to a) LOS search, b) COM, and c) NLOS search tasks. Additionally, on the right side of this diagram a bar chart indicating the PAP allocated to each task is also reported. Specifically, the maximum utility values are obtained with the allocation $PAP = [74, 435, 422, 103, 190, 248, 37]^T$ W $\cdot$ m^2, corresponding to a total PAP used by the MPAR of about 1509 W $\cdot$ m^2 (i.e., the sum of the maximum utility PAP values for each task).

Comparing the bar chart of Fig. 8 with the diagram representing the utility versus resource of Fig. 7, it is evident that in the case of normal operational conditions, all tasks are capable of obtaining the maximum utility. In this situation, therefore, independently of the task, the respective quality metric is greater than or

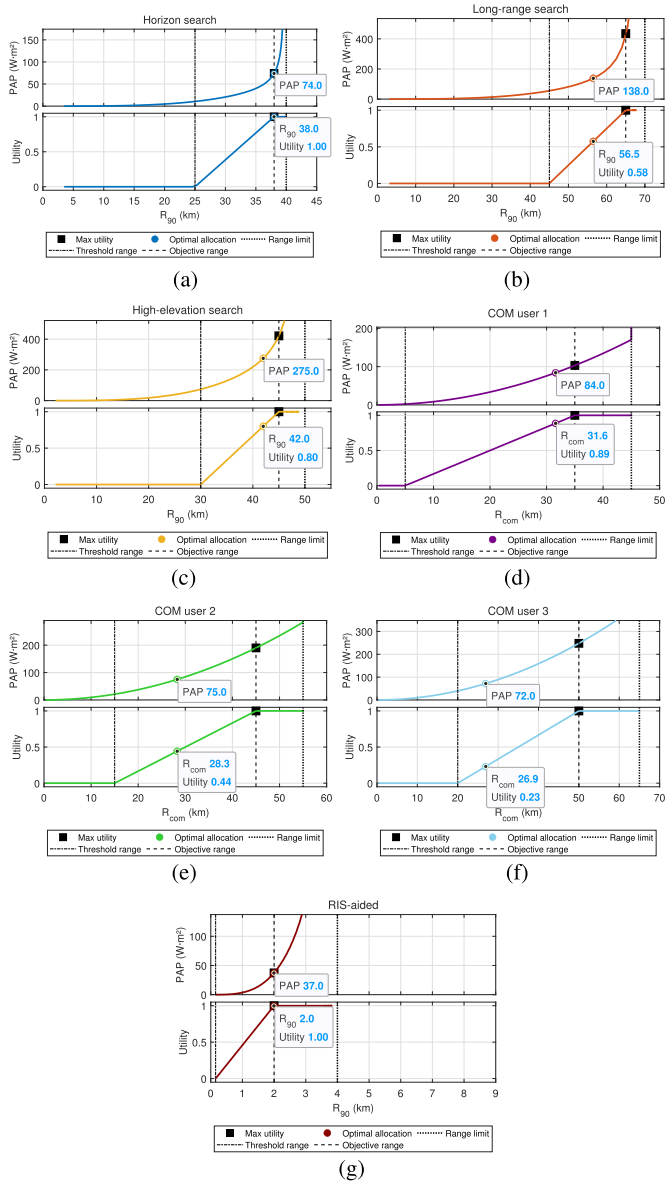

Fig. 10. Optimized resource allocation and utility of MPAR LOS search (subfigures a-c), COM (subfigures d-f), and NLOS search (subfigure g) tasks, with priority weights $\mathrm{w} = [0.4, 0.1, 0.2, 0.06, 0.06, 0.06, 0.12]^T$. (a) Horizon. (b) Long-range. (c) High-elevation. (d) COM user 1. (e) COM user 2. (f) COM user 3. (g) RIS-aided.

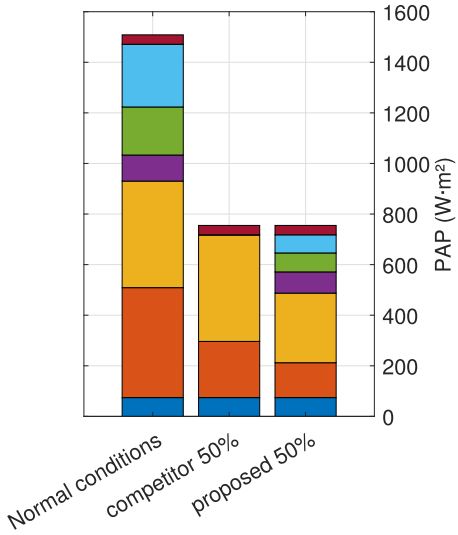

Fig. 11. Resource allocation of MPAR LOS search tasks, COM activities, and NLOS search operation, with priority weights $\mathrm{w} = [0.4, 0.1, 0.2, 0.06, 0.06, 0.06, 0.12]^T$. Comparison of the proposed algorithm with the competitor maximizing the weighted sum of SNRs.

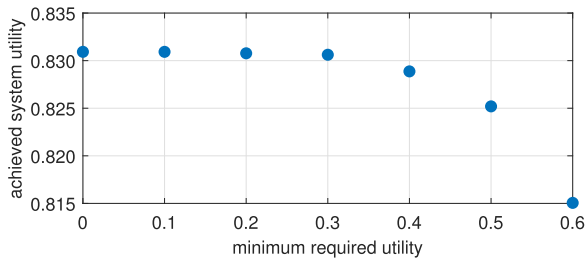

Fig. 12. Achieved objective function (2) versus minimum required utility (assumed equal for all the tasks).

equal to its desired objective value. However, in some operating conditions, the total amount of resources available at the MPAR cannot allow to assign the ideally required PAP to each task. This can be also explained observing that, often, a non negligible part of the available resources should be reserved to other tasks (e.g., tracking) [46]. For the above reasons, the RRM should compute the optimal PAP allocation, once its maximum available value is set. Hence, in this case study, the maximum PAP is set to the 50% of that under normal operational conditions, that is approximately 755 W $\cdot$ m^2. Moreover, the following set of priority weights is enforced, $\mathrm{w} = [0.4, 0.1, 0.2, 0.06, 0.06, 0.06, 0.12]^T$, providing low priorities to COM tasks with respect to search ones. Solving Problem (1) with the above constraints results in the resource distribution reported in Fig. 9, where as before subfigures refer to a) LOS search, b) COM, and c) NLOS search tasks. More specifically, the allocated PAPs are equal to $PAP = [74, 138, 275, 84, 75, 72, 37]^T$ W $\cdot$ m^2. To give insights into the obtained results, Fig. 10 shows for each task the optimal resource allocation in terms of PAP versus the R_{90} (respectively R_{com}) together with the corresponding utility, with subfigures referring to a)-c) LOS search, d)-f) COM, and g) NLOS search operations. As expected, the RRM allocates PAP so that the maximum utility is reached for the Horizon search function, being the task with highest priority, with a corresponding $R_{90} =$ 38 km. Analogously, also the RIS-aided search experiences an allocation of PAP that allows to reach the maximum utility with $R_{90} = 2$ km. This is because it has a medium priority (i.e., a weight 0.12) together with the fact that it has low requirements in terms of resource. The worst case is observed in the COM user 3 task where the PAP allocation only ensures a utility of 0.23, being its priority weight quite low and given by 0.06.

Now, the algorithm solving Problem (1) with the weighted sum of SNRs as objective function is considered as a possible competitor. In such a case, the optimization of the weighted

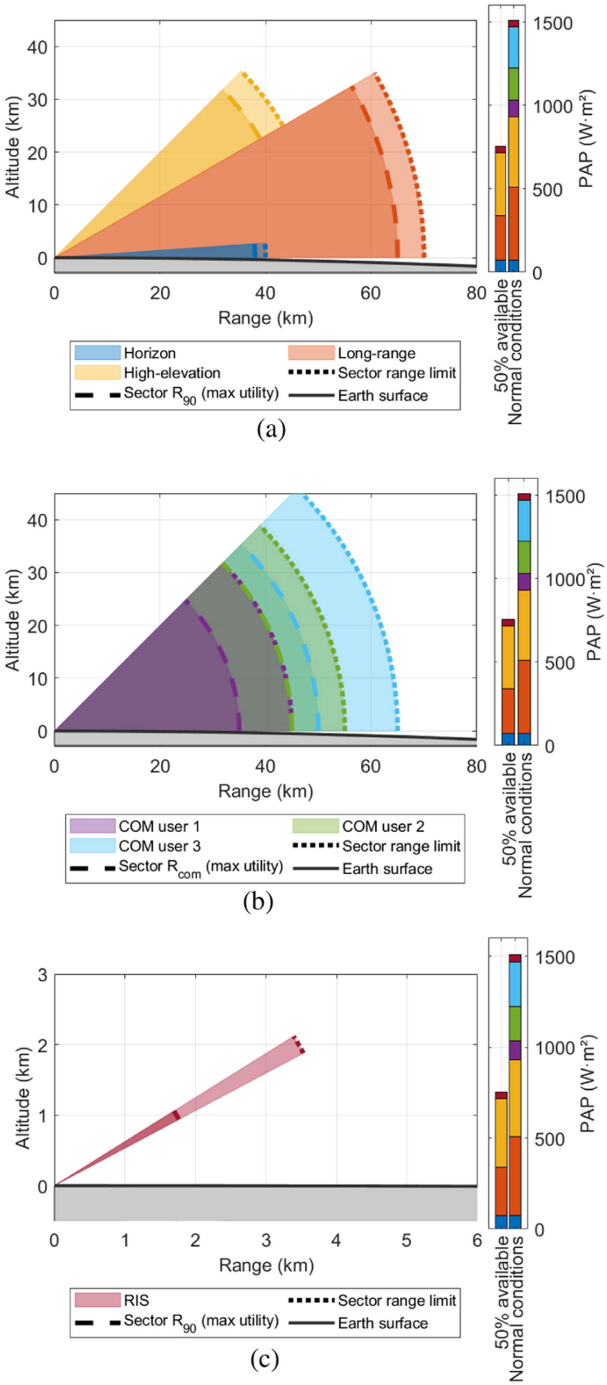

Fig. 13. Resource allocation of MPAR LOS search tasks (subfigure a), COM activities (subfigure b), and NLOS search operation (subfigure c), with priority weights $\mathrm{w} = [0.4, 0.20, 0.20, 0, 0, 0, 0.2]^T$.

SNR together with the linear constraints gives rise to a linear programming problem. Results are graphically reported in Fig. 11, where the competitor provides a PAP allocation, i.e., $PAP = [74, 222, 421, 0, 0, 0, 37]^T$ W · m^2, that substantially differs from that given by the proposed method, i.e., $PAP = [74, 138, 275, 84, 75, 72, 37]^T$ W · m^2. With the above allocation, the competitor reaches utilities equal to 1, 0.81, 1, 0, 0, 0, and 1, for the seven tasks, respectively, with an

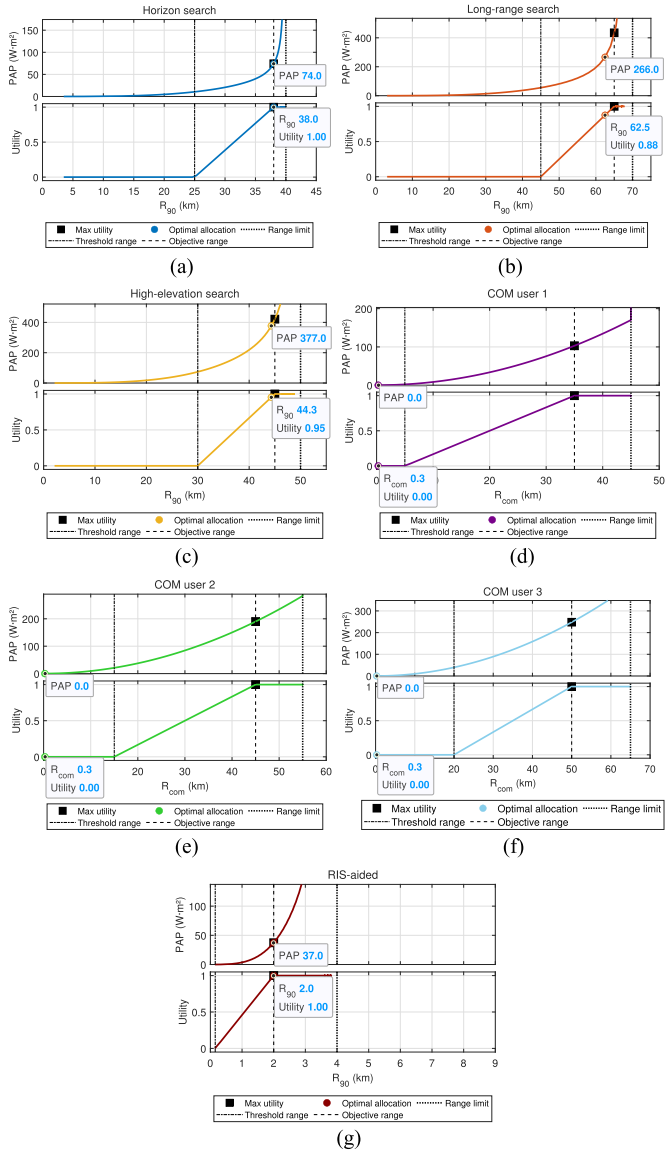

Fig. 14. Optimized resource allocation and utility of MPAR LOS search (subfigures a-c), COM (subfigures d-f), and NLOS search (subfigure g) tasks, with priority weights $\mathrm{w} = [0.4, 0.20, 0.20, 0, 0, 0, 0.2]^T$. (a) Horizon. (b) Long-range. (c) High-elevation. (d) COM user 1. (e) COM user 2. (f) COM user 3. (g) RIS-aided.

average utility of 0.801, whereas the proposed method provides as utility values 1, 0.58, 0.80, 0.89, 0.44, 0.23, and 1 with an average utility of 0.831. Analyzing these results it is clear that the competitor does not allocate any resources to the COM tasks with a corresponding zero utility. Differently, the proposed method is capable of allocating some resources to all tasks providing at least some non-zero utilities. Moreover, the average utility reached by the proposed method is higher than that of the competitor (the competitor experiences a loss of 3.6% in this case). Therefore, the validity and advantages of the proposed method should appear now much more evident.

To give further insights about the behavior of the proposed algorithm, the analysis of the case study 1 is repeated with a PAP requirement set so as to ensure a utility of 0.5 for

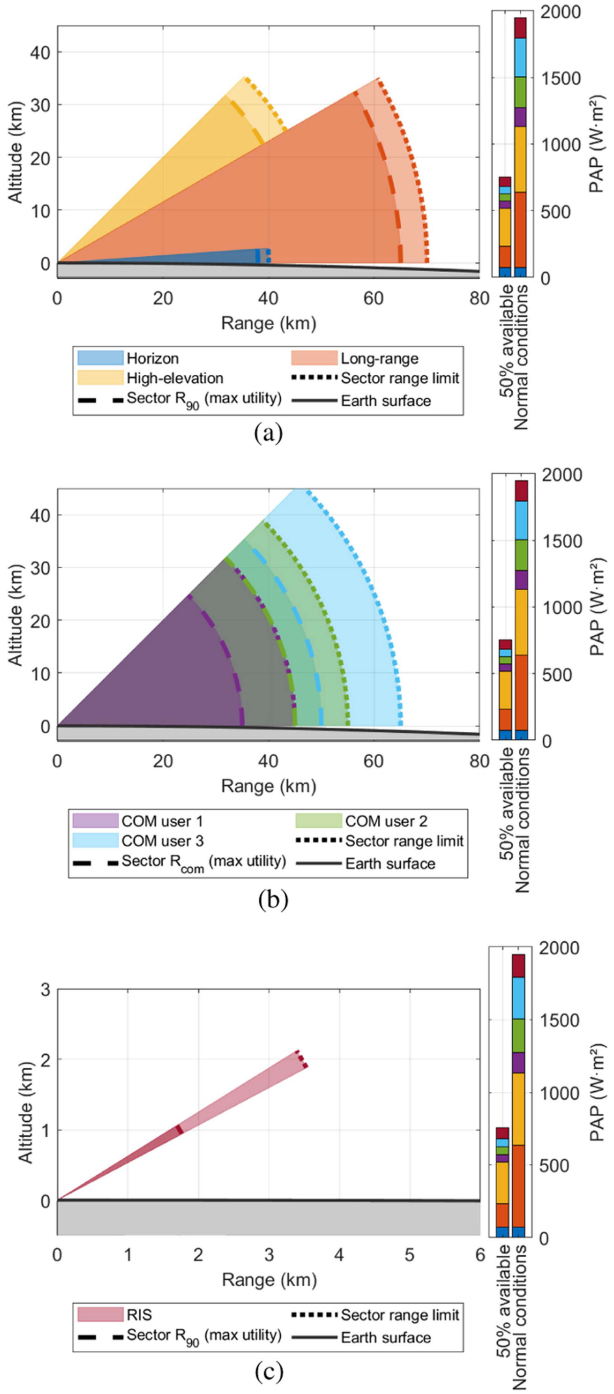

Fig. 15. Resource allocation of MPAR LOS search tasks (subfigure a), COM activities (subfigure b), and NLOS search operation (subfigure c), assuming the worst case scanning loss.

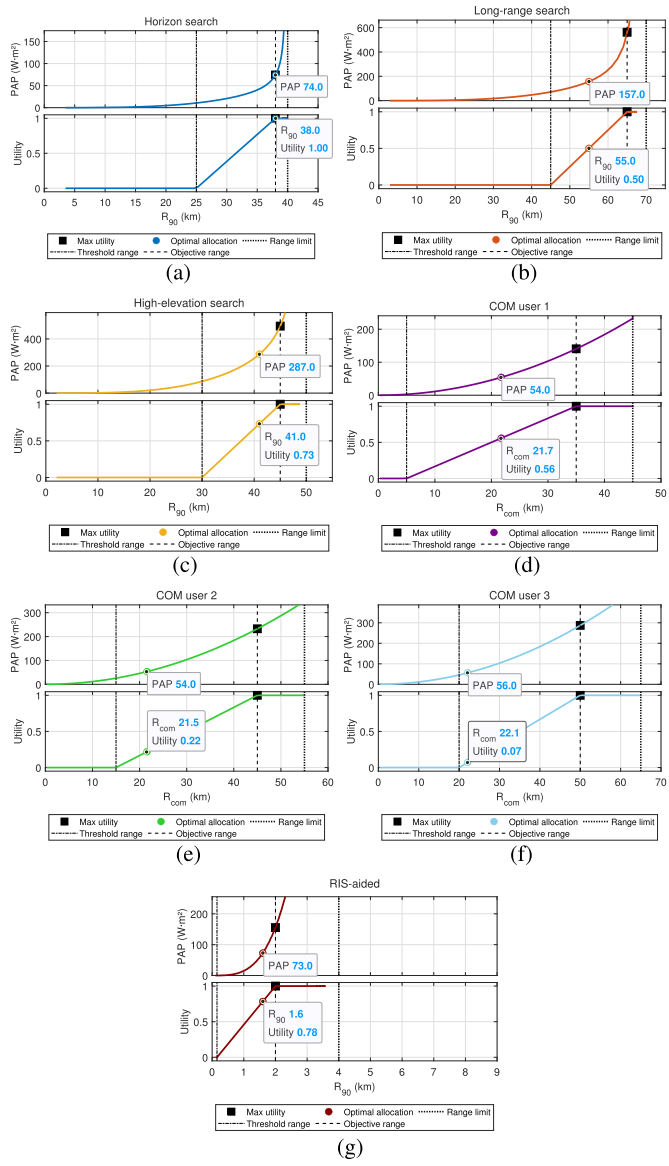

Fig. 16. Optimized resource allocation and utility of MPAR LOS search (subfigures a-c), COM (subfigures d-f), and NLOS search (subfigure g) tasks, assuming the worst case scanning loss. (a) Horizon. (b) Long-range. (c) High-elevation. (d) COM user 1. (e) COM user 2. (f) COM user 3. (g) RIS-aided.

each task, viz. $PAP_{\min} = [25, 122, 168, 34, 85, 122, 5]^T$ W $\cdot$ m^2. Solving Problem (1) results in the resource distribution $PAP = [74, 138, 245, 54, 85, 122, 37]^T$ W $\cdot$ m^2, with corresponding utilities equal to 1, 0.58, 0.73, 0.68, 0.50, 0.50, and 1, for the seven tasks, respectively. In such a case, the average utility is 0.825, whereas in the previous case without any guarantees on the minimum offered QoS it was 0.831. As expected enforcing additional requirements reduces the feasibility region (i.e., the available degrees of freedom) and possibly the resulting achieved objective function (2). Moreover, from the inspection of these results, the evidence is that the RRM allocates the PAP so that the maximum utility is reached for the Horizon search function, being it the task with highest priority. Similarly, the RIS is maintained invariant since it requires very low PAP. However, the RRM, accounting for a minimum ensured QoS to the different tasks, tends to sacrifice the High-elevation task, and COM user 1 that experience a loss in their achieved utility, to ensure that COM user 2 and 3 attain the minimum required PAP with utility 0.5. Definitely, when a non-zero lower bound on the PAP is considered, the MPAR is prone to subtract some resources to the (low weights) tasks whose allocation exceed the minimum requirements.

TABLE IV
SCANNING LOSS (EXPRESSED IN DB) FOR THE WORST ANTENNA POINTING DIRECTION CASE

HHorizon	Long-range	High-elevation	COM user 1-3	RIS
0.02	1.25	3.01	1.51	7.45

Before concluding this case study, Fig. 12 shows the objective function (2) achieved by the proposed algorithm versus the utility value (assumed equal among the different tasks). As expected, the allocation performed by the RRM attains a global utility that reduces as the constraints become more and more demanding.

C. Case Study 2

In this situation, the PAP allocation is performed for a different set of priority weights, again setting its maximum value to 755 W $\cdot$ m^2, i.e., half of that used under normal operational conditions. As a matter of fact, the priority weights for the COM tasks are fixed to 0, resulting in the vector $\mathrm{w} = [0.4, 0.2, 0.2, 0, 0, 0, 0.2]^T$. The solution to Problem (1) with the above constraints produces the PAP assignment over the considered tasks illustrated in Fig. 13, where subfigures refer to a) LOS search tasks, c) COM tasks, and d) RIS-aided search task. Specifically, the allocated PAP values are $PAP = [74, 266, 378, 0, 0, 0, 37]^T$ W $\cdot$ m^2. Again, Fig. 14 shows for each task the optimal resource distribution in terms of PAP versus R_{90} (respectively R_{com}) together with the corresponding utility, with subfigures referring to a)-c) LOS search tasks, d)-f) COM tasks, and g) RIS-aided search task. As expected the RRM does not allocate any PAP to the COM tasks reflecting the associated zero priority weights. On the contrary, the Long-range and High-elevation experience a growth in the assignment of their resources, with a consequent increment of utility that increases from 0.65 to 0.88 and from 0.83 to 0.95 w.r.t. the case study 1, respectively. Obviously, the other two tasks (namely, Horizon and RIS-aided search), having already reached their maximum utility, continue to maintain the same allocation as before.

D. Case Study 3

The test performed in this subsection is devoted to the impact of the antenna pointing direction on the performance of the MPAR in terms of resource distribution over the different tasks. In particular, for all tasks, the term accounting for scanning losses is fixed according to the values summarized in Table IV. Moreover, as to the other parameters, this study refers to the same simulation setting as in Section IV-B, apart for, as already specified losses accounting for the spatial selectivity of the antenna gain are set equal to their respective worst case for each angular sector.

The conducted test considers the availability of maximum PAP of 755 W $\cdot$ m^2 (that is again approximately the 50% of that under normal operational conditions in the case study 1), with the same priority weights as in the first case study. Solving Problem (1) with the above constraints results in the PAP assignment illustrated in Fig. 15, where subfigures refer to a) LOS search, c) COM, and d) RIS-aided search tasks. More in detail, the allocated PAPs are now equal to $PAP = [74, 157, 287, 54, 54, 56, 73]^T$ W $\cdot$ m^2, respectively. Again, to further shed light on the results, Fig. 16 shows for each task the optimal resource allocation in terms of PAP versus R_{90} (respectively R_{com}) along with their corresponding utility, with subfigures referring to a)-c) LOS search, d)-f) COM, and g) RIS-aided search tasks. It is now interesting to observe that the resource allocation does not follow the trend as in the scenario analyzed in Section IV-B. In fact, the COM tasks are all penalized with a reduction in the assignment of their PAP due to their very low priorities (i.e., 0.06). The majority of resources are allocated to the other tasks, with the Horizon search function that attains its maximum utility thanks to the attributed high priority. The RIS-aided search task also reaches a high utility of 0.78 because of a joint combination of a medium priority weight and a reduced PAP necessary to satisfy it. Finally, it is worth observing that all the considered tasks (except the Horizon) suffer the effect of the scanning loss that in turn reflects on a higher PAP that is required to reach the same utility. Therefore, the RRM tends to sacrifice the tasks with the lowest priority, i.e., COM ones, to guarantee sufficient performance to the others.

V. CONCLUDING REMARKS

This article has addressed the problem of optimal PAP allocation in a MPAR system performing ISAC operations. More specifically, the considered methodology has been aimed at solving the QoS optimization problem jointly accounting for search scenarios in LOS and NLOS as well as COM tasks. Therefore, to maximize the QoS, the resource allocation is formulated as a constrained optimization problem whose objective function is the weighted sum of the utilities achieved with the assigned PAP to each specific task. In this respect, the cumulative detection range is defined as a quality metric for search tasks, whereas for COM tasks it is chosen as the range ensuring a desired channel capacity per bandwidth. Several case studies have been analyzed to prove the validity of the designed allocation strategy in challenging operational scenarios, ranging from the analysis of different priority weights selections to the study of the impact of the spatial selectivity of the antenna pointing angle. From the analyses of the results, the evidence is that the MPAR tends to mostly allocate the available resources to the high priority tasks at the expense of the others. By doing so, it is ensured that the utilities for the most important tasks attain values close to their objectives, whereas for the remainder tasks a lower level of satisfaction is obtained.

Possible future researches could consider the extension of the framework to a multiface and/or multiband radar as well as to the multiradar systems. Moreover, the allocation of the beamformer weights to the different tasks is another valuable topic.

REFERENCES

[1] P. Moo and Z. Ding, *Adaptive Radar Resource Management*. Cambridge, MA, USA: Academic Press, 2015.
[2] D. Friedman, *The Double Auction Market: Institutions, Theories, and Evidence*. London, U.K.: Routledge, 2018.

[3] A. Charlish and F. Hoffmann, "Cognitive radar management," *Novel Radar Techn. Appl.: Waveform Diversity Cogn. Radar, Target Tracking Data Fusion*, vol. 2, pp. 157–193, 2017.
[4] R. Rajkumar, C. Lee, J. Lehoczky, and D. Siewiorek, "A resource allocation model for QoS management," in *Proc. IEEE Real-Time Syst. Symp.*, 1997, pp. 298–307.
[5] A. Charlish, K. Woodbridge, and H. Griffiths, "Agent based multifunction radar surveillance control," in *Proc. IEEE RadarCon*, 2011, pp. 824–829.
[6] A. B. Charlish, "Autonomous agents for multi-function radar resource management," Ph.D. dissertation, UCL (University College London), 2011.
[7] C.-F. Kuo, T.-W. Kuo, and C. Chang, "Real-time digital signal processing of phased array radars," *IEEE Trans. Parallel Distrib. Syst.*, vol. 14, no. 5, pp. 433–446, May 2003.
[8] C.-S. Shih, S. Gopalakrishnan, P. Ganti, M. Caccamo, and L. Sha, "Scheduling real-time dwells using tasks with synthetic periods," in *Proc. 24th IEEE Real-Time Syst. Symp.*, 2003, pp. 210–219.
[9] C.-S. Shih, S. Gopalakrishnan, P. Ganti, M. Caccamo, and L. Sha, "Template-based real-time dwell scheduling with energy constraint," in *Proc. 9th IEEE Real-Time Embedded Technol. Appl. Symp.*, 2003, pp. 19–27.
[10] J. P. Hansen, S. Ghosh, R. Rajkumar, and J. Lehoczky, "Resource management of highly configurable tasks," in *Proc. 18th Int. Parallel Distrib. Process. Symp.*, 2004, pp. 1–8.
[11] J. Hansen, R. Rajkumar, J. Lehoczky, and S. Ghosh, "Resource management for radar tracking," in *Proc. IEEE Conf. Radar*, 2006, pp. 140–147.
[12] S. Ghosh, R. Raj Rajkumar, J. Hansen, and J. Lehoczky, "Integrated QoS-Aware resource management and scheduling with multi-resource constraints," *Real-Time Syst.*, vol. 33, pp. 7–46, 2006.
[13] F. Hoffmann and A. Charlish, "A resource allocation model for the radar search function," in *Proc. IEEE Int. Radar Conf.*, 2014, pp. 1–6.
[14] A. Charlish, K. Woodbridge, and H. Griffiths, "Multi-target tracking control using continuous double auction parameter selection," in *Proc. IEEE 15th Int. Conf. Inf. Fusion*, 2012, pp. 1269–1276.
[15] A. Charlish and F. Katsilieris, "Array Radar Resource Management," *Novel Radar Techn. Appl.: Real Aperture Array Radar, Imag. Radar, Passive Multistatic Radar*, vol. 1, pp. 135–171, 2017.
[16] A. Charlish, F. Hoffmann, C. Degen, and I. Schlangen, "The development from adaptive to cognitive radar resource management," *IEEE Aerosp. Electron. Syst. Mag.*, vol. 35, no. 6, pp. 8–19, Jun. 2020.
[17] A. Ahmed, Y. D. Zhang, and B. Himed, "Distributed dual-function radar-communication MIMO system with optimized resource allocation," in *Proc. IEEE Radar Conf. (RadarConf)*, 2019, pp. 1–5.
[18] C. Shi, Y. Wang, F. Wang, S. Salous, and J. Zhou, "Power resource allocation scheme for distributed MIMO dual-function radar-communication system based on low probability of intercept," *Digit. Signal Process.*, vol. 106, 2020, Art. no. 102850.
[19] L. Wu, K. V. Mishra, M. B. Shankar, and B. Ottersten, "Resource allocation in heterogeneously-distributed joint radar-communications under asynchronous bayesian tracking framework," *IEEE J. Sel. Areas Commun.*, vol. 40, no. 7, pp. 2026–2042, Jul. 2022.
[20] F. Liu et al., "Integrated sensing and communications: Towards dual-functional wireless networks for 6G and beyond," *IEEE J. Sel. Areas Commun.*, vol. 40, no. 6, pp. 1728–1767, Jun. 2022.
[21] J. Wang, N. Varshney, C. Gentile, S. Blandino, J. Chuang, and N. Golmie, "Integrated sensing and communication: Enabling techniques, applications, tools and data sets, standardization, and future directions," *IEEE Internet Things J.*, vol. 9, no. 23, pp. 23416–23440, Dec. 2022.
[22] S. P. Chepuri, N. Shlezinger, F. Liu, G. C. Alexandropoulos, S. Buzzi, and Y. C. Eldar, "Integrated sensing and communications with reconfigurable intelligent surfaces," 2022, *arXiv:2211.01003*.
[23] J. Zhang, N. Garg, and T. Ratnarajah, "In-band-Full-Duplex integrated sensing and communications for IAB networks," *IEEE Trans. Veh. Technol.*, vol. 71, no. 12, pp. 12782–12796, Dec. 2022.
[24] H. Luo, R. Liu, M. Li, and Q. Liu, "RIS-aided integrated sensing and communication: Joint beamforming and reflection design," *IEEE Trans. Veh. Technol.*, vol. 72, no. 7, pp. 9626–9630, Jul. 2023.
[25] Q. Zhu, M. Li, R. Liu, and Q. Liu, "Joint transceiver beamforming and reflecting design for active RIS-aided ISAC systems," *IEEE Trans. Veh. Technol.*, vol. 72, no. 7, pp. 9636–9640, Jul. 2023.
[26] J. D. Mallett and L. E. Brennan, "Cumulative probability of detection for targets approaching a uniformly scanning search radar," *Proc. IEEE*, vol. 51, no. 4, pp. 596–601, Apr. 1963.
[27] M. A. Richards, J. Scheer, W. A. H., and W. L. Melvin, *Principles of Modern Radar*, vol. 1. Citeseer, 2010.
[28] E. S. Elliott, "Beamwidth and directivity of large scanning arrays," *Part Two, Microw. J.*, pp. 74–82, 1964.
[29] H. L. Van Trees, *Optimum Array Processing: Part IV of Detection, Estimation, and Modulation Theory*. Hoboken, NJ, USA: Wiley, 2002.
[30] J. Marcum, "A statistical theory of target detection by pulsed radar," *IRE Trans. Inf. Theory*, vol. 6, no. 2, pp. 59–267, 1960.
[31] A. Aubry, A. De Maio, and M. Rosamilia, "Reconfigurable intelligent surfaces for N-LOS radar surveillance," *IEEE Trans. Veh. Technol.*, vol. 70, no. 10, pp. 10735–10749, Oct. 2021.
[32] Z. Yang, Y. Liu, Y. Chen, and N. Al-Dhahir, "Machine learning for user partitioning and phase shifters design in RIS-Aided NOMA networks," *IEEE Trans. Commun.*, vol. 69, no. 11, pp. 7414–7428, Nov. 2021.
[33] G. Zhou, C. Pan, H. Ren, K. Wang, M. Elkashlan, and M. D. Renzo, "Stochastic learning-based robust beamforming design for RIS-Aided millimeter-wave systems in the presence of random blockages," *IEEE Trans. Veh. Technol.*, vol. 70, no. 1, pp. 1057–1061, Jan. 2021.
[34] A. S. Abdalla and V. Marojevic, "Aerial RIS for MU-MISO: Joint base station beamforming and RIS phase shifter optimization," in *Proc. IEEE Int. Conf. Sensing, Commun., Netw.*, 2022, pp. 19–24.
[35] R. Hashemi, S. Ali, N. H. Mahmood, and M. Latva-Aho, "Deep reinforcement learning for practical phase-shift optimization in RIS-Aided MISO URLLC systems," *IEEE Internet Things J.*, vol. 10, no. 10, pp. 8931–8943, Oct. 2023.
[36] S.-K. Chou, O. Yurduseven, H. Q. Ngo, and M. Matthaiou, "On the aperture efficiency of intelligent reflecting surfaces," *IEEE Wireless Commun. Lett.*, vol. 10, no. 3, pp. 599–603, Mar. 2020.
[37] P. Viswanath, D. N. C. Tse, and R. Laroia, "Opportunistic beamforming using dumb antennas," *IEEE Trans. Inf. Theory*, vol. 48, no. 6, pp. 1277–1294, Jun. 2002.
[38] D. Tse and P. Viswanath, *Fundamentals of Wireless Communication*. Cambridge, MA, USA: Cambridge Univ. Press, 2005.
[39] M. Kountouris, "Multiuser multi-antenna systems with limited feedback," Ph.D. dissertation, Télécom ParisTech, 2008.
[40] "Find minimum of constrained nonlinear multivariable function," [Online]. Available: https://it.mathworks.com/help/optim/ug/fmincon.html?s_tid=doc_ta,MathworksMatlab
[41] R. H. Byrd, M. E. Hribar, and J. Nocedal, "An interior point algorithm for large-scale nonlinear programming," *SIAM J. Optim.*, vol. 9, no. 4, pp. 877–900, 1999.
[42] R. H. Byrd, J. C. Gilbert, and J. Nocedal, "A trust region method based on interior point techniques for nonlinear programming," *Math. Prog.*, vol. 89, pp. 149–185, 2000.
[43] R. A. Waltz, J. L. Morales, J. Nocedal, and D. Orban, "An interior algorithm for nonlinear optimization that combines line search and trust region steps," *Math. Prog.*, vol. 107, no. 3, pp. 391–408, 2006.
[44] "Quality-of-service optimization for radar resource management," [Online]. Available: https://it.mathworks.com/help/radar/ug/quality-of-service-optimization-for-resource-management-in-multifunction-phased-array-radar.html, *Mathworks Matlab*.
[45] E. Arkoumaneas, "Effectiveness of a ground jammer," in *Proc. IEE Proc. F. (Commun., Radar Signal Process.)*, vol. 129, no. 3, 1982, pp. 202–207.
[46] D. K. Barton, *Radar Equations for Modern Radar*. Norwood, MA, USA: Artech House, 2013.

Augusto Aubry (Senior Member, IEEE) received the Dr.Eng. degree in telecommunication engineering (with Hons.) and the Ph.D. degree in electronic and telecommunication engineering from the University of Naples Federico II, Naples, Italy, in 2007 and 2011, respectively. From February to April 2012, he was a Visiting Researcher with the Hong Kong Baptist University, Hong Kong. He is currently an Associate Professor with the University of Naples Federico II. His research interests include statistical signal processing and optimization theory, with emphasis on MIMO communications and radar signal processing. He was also the co-recipient of the 2013 Best Paper Award (entitled to B. Carlton) of IEEE TRANSACTIONS ON AEROSPACE AND ELECTRONIC SYSTEMS with the contribution "Knowledge-Aided (Potentially Cognitive) Transmit Signal and Receive Filter Design in Signal-Dependent Clutter". Dr. Aubry was the Recipient of the 2022 IEEE Fred Nathanson Memorial Award as the young (less than 40 years of age) AESS Radar Engineer 2022, with the following citation "For outstanding contributions to the application of modern optimization theory to radar waveform design and adaptive signal processing."

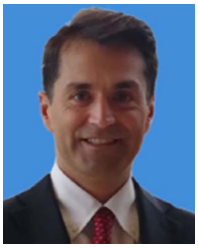

Antonio De Maio (Fellow, IEEE) received the Dr.Eng. (Hons.) and Ph.D. degrees in information engineering from the University of Naples Federico II, Naples, Italy, in 1998 and 2002, respectively. From October to December 2004, he was a Visiting Researcher with the U.S. Air Force Research Laboratory, Rome, NY, USA. From November to December 2007, he was a Visiting Researcher with The Chinese University of Hong Kong, Hong Kong. He is currently a Professor with the University of Naples Federico II. His research interest include the field of statistical signal processing, with emphasis on radar detection, optimization theory applied to radar signal processing, and multiple-access communications. He was the recipient of the 2010 IEEE Fred Nathanson Memorial Award as the young (less than 40 years of age) AESS Radar Engineer 2010 whose performance is particularly noteworthy as evidenced by contributions to the radar art over a period of several years, with the following citation for "robust CFAR detection, knowledge-based radar signal processing, and waveform design and diversity". He was the co-recipient of the 2013 Best Paper Award (entitled to B. Carlton) of the IEEE TRANSACTIONS ON AEROSPACE AND ELECTRONIC SYSTEMS with the contribution "Knowledge-Aided (Potentially Cognitive) Transmit Signal and Receive Filter Design in Signal-Dependent Clutter."

Luca Pallotta (Senior Member, IEEE) received the Laurea Specialistica degree (*cum laude*) in telecommunication engineering from the University of Sannio, Benevento, Italy, in 2009, and the Ph.D. degree in electronic and telecommunication engineering from the University of Naples Federico II, Naples, Italy, in 2014. From 2019 to 2022, he was an Assistant Professor with the University of Roma Tre, Rome, Italy. He is currently an Assistant Professor with the University of Basilicata, Potenza, Italy. His research interests include the field of statistical signal processing, with emphasis on radar/SAR signal processing, radar targets detection and classification, and polarimetric radar/SAR. Since November 2020, he has been an Associate Editor for IEEE JOURNAL OF SELECTED TOPICS IN APPLIED EARTH OBSERVATIONS AND REMOTE SENSING. From July 2018 to February 2021, he was an Associate Editor for the *Journal Springer Signal, Image and Video Processing*. Dr. Pallotta was the recipient of the Student Paper Competition at the IEEE Radar Conference 2013.

Open Access funding provided by 'Università degli Studi di Napoli "Federico II"' within the CRUI CARE Agreement